

Structure and Dynamics of a Compressed Dihydride Complex of Osmium

Nils Schloerer,^{†,1} Vincent Pons,[†] Dmitry G. Gusev,^{*,‡} and D. Michael Heinekey^{*,†}

Departments of Chemistry, University of Washington, Box 351700, Seattle, Washington 98195-1700, and Wilfred Laurier University, Waterloo, Ontario N2L 3C5, Canada

Received March 30, 2006

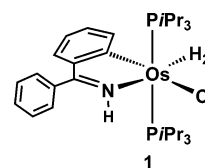
The complex $\text{OsCl}(\text{NH}=\text{C}(\text{Ph})\text{C}_6\text{H}_4)(\text{P}i\text{Pr}_3)_2(\text{H}_2)$ (**1**) has been characterized by Esteruelas and co-workers (*Organometallics* **1998**, *17*, 4065–4076) as an elongated dihydrogen complex based on relaxation time measurements and observation of $J_{\text{H-D}} = 6.3$ Hz in **1-d**₁. Variable-temperature NMR studies were reported in which the single hydride resonance observed at ambient temperature decoalesced into two signals at low temperature (193 K), which was attributed to hindered rotation of the bound H_2 ligand. Reinvestigation of the low-temperature NMR spectra of **1** reveals a more complex situation. Examination of the ¹H and ³¹P NMR spectra of **1** and **1-d**₁ at lower temperatures than previously studied demonstrates that quantum mechanical exchange coupling is observed between the metal-bonded hydrogen atoms. This coupling is quenched in **1-d**₁. Hindered rotation around Os–P bonds in **1** also contributes to the observed NMR spectra.

Introduction

The coordination chemistry of dihydrogen has developed very rapidly into an active field of study, with fascinating structural variability and interesting dynamic behavior demonstrated by bound dihydrogen.² The well-accepted bonding description for the binding of dihydrogen invokes electron donation from the σ bond into a metal acceptor orbital and back-donation from filled metal d orbitals into the σ^* orbital of H_2 . This model resembles the one used to describe the binding of ethylene in transition metal complexes. In contrast to ethylene, barriers to rotation of bound H_2 are generally very small (1–2 kcal/mol) and are usually observed by inelastic neutron scattering.³ Significant rotational barriers (7–10 kcal/mol) have been reported for a small number of metal H_2 complexes with formal d² configurations, where electronic asymmetry leads to higher barriers to rotation.⁴

An apparent exception to this generalization is provided by $\text{OsCl}(\text{NH}=\text{C}(\text{Ph})\text{C}_6\text{H}_4)(\text{P}i\text{Pr}_3)_2(\text{H}_2)$ (**1**), reported by Esteruelas

and co-workers (bromide and iodide analogues were also reported to have similar properties).⁵



Relaxation time measurements on the hydride resonance of **1** at -6.5 ppm gave a $T_{1(\text{min})}$ value of 49 ms at 233 K (300 MHz), corresponding to an H–H distance of ca. 1.36 Å. In **1-d**₁, $J_{\text{HD}} = 6.3$ Hz was reported. On the basis of these observations, complex **1** was formulated as an elongated dihydrogen complex of Os(II) with a d⁶ configuration. In the ¹H NMR spectrum at low temperatures, the hydride resonance of **1** was reported to broaden and ultimately decoalesce into two broad resonances of equal intensity at 193 K. The ³¹P NMR spectrum of **1** was reported to be invariant with temperature.

These observations were quite reasonably interpreted in terms of the presence of an elongated dihydrogen ligand exhibiting hindered rotation. As noted above, significant barriers to rotation have generally not been reported in complexes with d⁶ configurations, so we found these results to be intriguing.

We have reinvestigated the structure of complex **1** using ¹H and ³¹P NMR spectroscopy. The range of temperatures studied has been extended below that previously reported. Our observations suggest that the structure and dynamic behavior of **1** presents a more complex situation than initially thought.

Experimental Section

Complex **1** was prepared as previously reported. NMR spectra were obtained at 500 and 750 MHz on Bruker Avance spectrometers running xwinnmr 2.6 or 3.5. Low-temperature measurements were

(5) Barea, G.; Esteruelas, M. A.; Lledós, A.; López, A. M.; Oñate, E.; Tolosa, J. I. *Organometallics* **1998**, *17*, 4065–4076.

[†] University of Washington.

[‡] Wilfred Laurier University.

(1) Current address: Institute for Organic Chemistry, University of Cologne, Greinstrasse 4, 50939 Cologne, Germany.

(2) Kubas, G. J. *Metal Dihydrogen and σ -Bond Complexes: Structure, Theory and Reactivity*; Kluwer Academic/Plenum Publishers: New York, 2001.

(3) Eckert, J. *Spectrochim. Acta A* **1992**, *48*, 363–378.

(4) (a) Sabo Etienne, S.; Chaudret, B.; El Makarim, H. A.; Barthelat, J. C.; Daudey, J. P.; Moïse, C.; Leblanc, J. C. *J. Am. Chem. Soc.* **1994**, *116*, 9335. (b) Jalon, F.; Manzano, B.; Otero, A.; Villasenor, E.; Chaudret, B. *J. Am. Chem. Soc.* **1995**, *117*, 10123. (c) Sabo-Etienne, S.; Chaudret, B.; El Makarim, H. A.; Barthelat, J. C.; Daudey, J. P.; Ulrich, P.; Limbach H. H.; Moïse, C. *J. Am. Chem. Soc.* **1995**, *117*, 11602. (d) Antinolo, A.; Carrillo Hermosilla, F.; Fajardo, M.; García Yuste, S.; Otero, A.; Camanyes, S.; Maseras, F.; Moreno, M.; Lledós, A.; Lluch, J. M. *J. Am. Chem. Soc.* **1997**, *119*, 6107. (e) Camanyes, S.; Maseras, F.; Moreno, M.; Lledós, A.; Lluch, J. M.; Bertrán, J. *Chem. Eur. J.* **1999**, *5* (4), 1166–1171. (f) Sabo-Etienne, S.; Rodriguez, V.; Donnadiu, B.; Chaudret, B.; El Makarim, H. A.; Barthelat, J. C.; Ulrich, P.; Limbach H. H.; Moïse, C. *New J. Chem.* **2001**, *25*, 55–62. (g) Pons, V.; Conway, S. L. J.; Green, M. L. H.; Green, J. C.; Herbert, B. J.; Heinekey, D. M. *Inorg. Chem.* **2004**, *43*, 3475–3483.

made by cooling the probe with a stream of cold N₂ (g) from a liquid N₂ boil off evaporator. CDFCl₂ and CDF₂Cl were prepared by the method of Siegel and Anet.⁶ NMR spectra were simulated using gNMR 4.1 (Ivorysoft).

The DFT calculations were carried out using Gaussian 03.⁷ The following basis sets were employed: BS1 included SDD (with the ECP) for Os, 6-31g(d, p) for all metal-bonded atoms, and 3-21g for the rest of the atoms; BS2 included SDD (with the ECP) for Os, 6-311g(d) for the N, P, and Cl atoms, 6-31g(p) for the Os–H and N–H hydrogens, and 6-31g(d) for all other atoms.⁸ The geometries of *c*-**1a** and *c*-**1b** (*c* denotes calculated) were fully optimized without constraints at the *m*PW1PW91/BS1 and *m*PW1PW91/BS2 levels, using the functional that included modified Perdew–Wang exchange and Perdew–Wang 91 correlation.⁹ The transition states **1-ts'** and **1-ts''** were both optimized at the *m*PW1K/BS1 and *m*PW1K/BS2 levels.¹⁰ Full geometry optimizations and a frequency calculation for *c*-**1a** were also carried out using the *m*PW1K functional. The nature of the stationary points *c*-**1a**, *c*-**1b**, **1-ts'**, and **1-ts''** was verified by frequency calculations, using the basis set BS1. The energies reported in this work were obtained by adding the zero-point energies calculated with BS1 to the corresponding SCF energies calculated with BS2. The relaxed potential energy scan for *c*-**1a** was performed at the *m*PW1PW91/BS1 level.

Results

NMR Spectroscopy. Complexes **1** and **1-d**₁ were prepared by the published procedure.⁵ As reported previously, the ambient-temperature ¹H NMR spectrum of **1** in the hydride region (CD₂Cl₂) consists of a single triplet resonance at –6.50 ppm (*J*_{H–P} = 13 Hz). An additional small coupling (ca. 3 Hz) to the N–H proton of the ligand is partially resolved. Lower temperature spectra obtained in CDFCl₂/CDF₂Cl mixtures exhibit line broadening and decoalescence into two broad resonances when the temperature is lowered to ca. 200 K. Further cooling causes each of these two resonances to further broaden and ultimately decoalesce into two distinct signals,

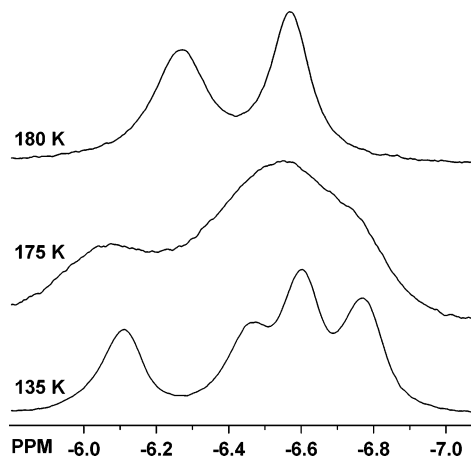


Figure 1. Partial (hydride region) ¹H NMR spectrum (500 MHz) of complex **1** in CDFCl₂/CDF₂Cl.

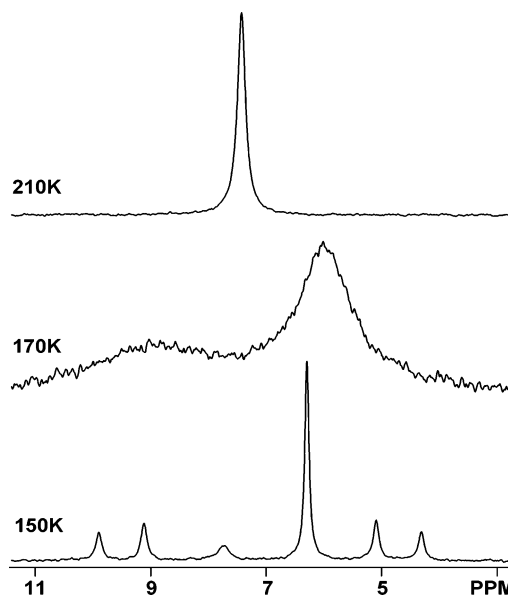


Figure 2. ³¹P{¹H} NMR spectrum (300 MHz) of complex **1** in CDFCl₂/CDF₂Cl.

giving a total of four hydride resonances at the lowest accessible temperatures (see Figure 1).

In the ambient-temperature ³¹P{¹H} NMR spectrum of **1**, a single resonance is observed at 6.8 ppm, which is consistent with the previous report. A spectrum acquired with selective decoupling of the aliphatic protons reveals a triplet resonance with *J*_{H–P} = 13 Hz. Lower temperature ³¹P{¹H} spectra reveal complex dynamic behavior (see Figure 2). At the lowest observation temperature (150 K), two major species are present. The predominant species exhibits a single ³¹P resonance at 6.2 ppm, while the minor species gives an AB pattern with $\delta_A = 9.5$ ppm, $\delta_B = 4.5$ ppm, and *J*_{A–B} = 240 Hz.

A heavily deuterated sample of **1** was prepared by reaction of **1** with methanol-*d*₄. Consistent with previous reports, the ¹H NMR spectrum of **1-d**₁ recorded with ³¹P decoupling at near ambient temperature exhibits a poorly resolved 1:1:1 pattern with *J*_{H–D} = 6.5 Hz. At very low temperature (155 K), two pairs of hydride resonances with a 55:45 intensity ratio are observed. The major species exhibits resonances at –5.4 and –7.9 ppm, while the minor species has resonances at –4.8 and –7.8 ppm (see Figure 3). The major species is designated **1a**, while the minor species is referred to as **1b**.

(6) Siegel, J. S.; Anet, F. A. L. *J. Org. Chem.* **1988**, *53*, 2629–2630.

(7) Frisch, M. J.; Trucks, G. W.; Schlegel, H. B.; Scuseria, G. E.; Robb, M. A.; Cheeseman, J. R.; Montgomery, J. A., Jr.; Vreven, T.; Kudin, K. N.; Burant, J. C.; Millam, J. M.; Iyengar, S. S.; Tomasi, J.; Barone, V.; Mennucci, B.; Cossi, M.; Scalmani, G.; Rega, N.; Petersson, G. A.; Nakatsuji, H.; Hada, M.; Ehara, M.; Toyota, K.; Fukuda, R.; Hasegawa, J.; Ishida, M.; Nakajima, T.; Honda, Y.; Kitao, O.; Nakai, H.; Klene, M.; Li, X.; Knox, J. E.; Hratchian, H. P.; Cross, J. B.; Bakken, V.; Adamo, C.; Jaramillo, J.; Gomperts, R.; Stratmann, R. E.; Yazyev, O.; Austin, A. J.; Cammi, R.; Pomelli, C.; Ochterski, J. W.; Ayala, P. Y.; Morokuma, K.; Voth, G. A.; Salvador, P.; Dannenberg, J. J.; Zakrzewski, V. G.; Dapprich, S.; Daniels, A. D.; Strain, M. C.; Farkas, O.; Malick, D. K.; Rabuck, A. D.; Raghavachari, K.; Foresman, J. B.; Ortiz, J. V.; Cui, Q.; Baboul, A. G.; Clifford, S.; Cioslowski, J.; Stefanov, B. B.; Liu, G.; Liashenko, A.; Piskorz, P.; Komaromi, I.; Martin, R. L.; Fox, D. J.; Keith, T.; Al-Laham, M. A.; Peng, C. Y.; Nanayakkara, A.; Challacombe, M.; Gill, P. M. W.; Johnson, B.; Chen, W.; Wong, M. W.; Gonzalez, C.; Pople, J. A. *Gaussian 03*, Revision B.05; Gaussian, Inc.: Wallingford, CT, 2004.

(8) For more information about basis sets implemented in Gaussian 03 and references see: Frish, A.; Frish, M. J.; Trucks, G. W. *Gaussian 03 User's Reference*; Gaussian, Inc.: Pittsburgh, PA, 2003. The basis sets are also available from the Extensible Computational Chemistry Environment Basis Set Database, which is developed and distributed by the Molecular Science Computing Facility, Environmental and Molecular Sciences Laboratory, which is part of the Pacific Northwest Laboratory, P.O. Box 999, Richland, WA 99352 (www.emsl.pnl.gov/forms/basisform.html).

(9) (a) Adamo, C.; Barone, V. *J. Chem. Phys.* **1998**, *108*, 664. (b) Perdew, J. P.; Burke, K.; Wang, Y. *Phys. Rev. B* **1996**, *54*, 16533. (c) Burke, K.; Perdew, J. P.; Wang, Y. In *Electronic Density Functional Theory: Recent Progress and New Directions*; Dobson, J. F., Vignale, G., Das, M. P., Eds.; Plenum: New York, 1998.

(10) (a) Lynch, B. J.; Fast, P. L.; Harris, M.; Truhlar, D. G. *J. Phys. Chem. A* **2000**, *104*, 4811. (b) Zhao, Y.; Pu, J.; Lynch, B. J.; Truhlar, D. G. *Phys. Chem. Chem. Phys.* **2004**, *6*, 673.

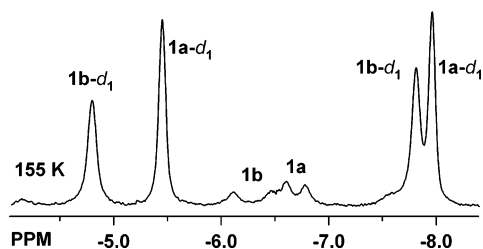


Figure 3. Partial (hydride region) ^1H NMR spectrum of a heavily deuterated sample of complex **1** in $\text{CDFCl}_2/\text{CDF}_2\text{Cl}$ at 155 K.

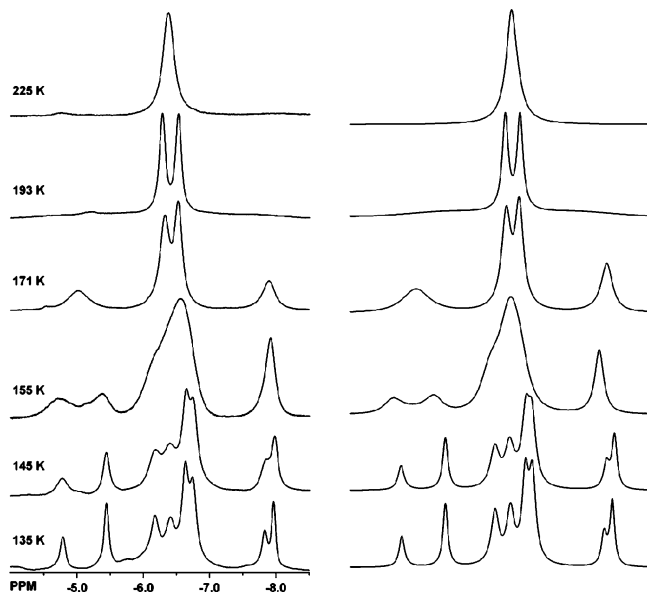


Figure 4. Partial (hydride region) ^1H NMR spectrum of a sample of complexes **1** and **1-d₁**: observed (left); simulated (right).

A partially deuterated sample of **1** was prepared and studied at a variety of temperatures in an effort to probe for isotope effects on the dynamic processes. The resulting ^1H NMR spectra are shown in Figure 4. The model used to calculate the spectra is described in the discussion section below.

Computational Studies

Structures for **1a** and **1b** were computed using DFT calculations. The approximately C_s symmetrical crystal structure of **1** reported by Esteruelas and co-workers⁵ is consistent with **1a** possessing equivalent phosphines. The crystal structure of **1** and the DFT-optimized calculated structure *c-1a* are shown in Figure 5. The PiPr_3 ligands of *c-1a* are in an eclipsed conformation, and the molecule is expected to have effective mirror symmetry in solution. The bond distances and angles involving Os and the non-hydrogen atoms agree well in the experimental and computed geometries; the largest difference is found for the Os–Cl bond, which is longer by 0.036 Å in *c-1a*.

A search of the Cambridge structural database for seven-coordinate compounds possessing inequivalent PiPr_3 ligands returned several molecules related to **1**. This structural information, and particularly the crystal structure of $\text{OsH}_2\text{Cl}(\kappa\text{-O,N-C}_6\text{H}_5\text{NO})(\text{PiPr}_3)_2$,¹¹ helped to develop a plausible model for **1b**. An optimization of this model resulted in structure *c-1b* presented in Figure 6. An inspection of the calculated structure reveals that *c-1b* is related to *c-1a* by rotation of a PiPr_3 ligand around the Os–P2 axis. The two phosphines are staggered in

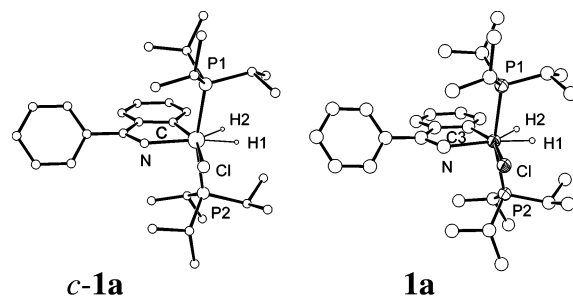


Figure 5. Theoretical (left) and experimental (right) structures of **1a**. C–H hydrogens are not shown for clarity. Thermal ellipsoids are drawn at 30% probability. Selected experimental bond distances [Å] and angles [deg]: Os–H1 1.53(4), Os–H2 1.42(4), Os–C3 2.069(4), Os–N 2.097(3), Os–Cl 2.482(1), Os–P1 2.387(1), Os–P2 2.381(1), H1–Os–H2 49(2), H1–Os–Cl 82(1), H2–Os–C3 72(2), N–Os–Cl 82.5(1), P1–Os–P2 162.31(4). Calculated bond distances [Å] and angles [deg]: Os–H1 1.617, Os–H2 1.588, Os–C 2.074, Os–N 2.119, Os–Cl 2.518, Os–P1 2.404, Os–P2 2.408, H1–Os–H2 54.2, H1–Os–Cl 76.9, H2–Os–C 70.9, N–Os–Cl 83.1, P1–Os–P2 164.1.

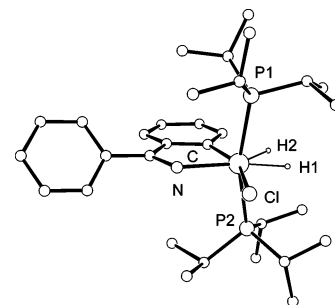


Figure 6. Calculated structure of *c-1b*. Hydrogen atoms bonded to carbon are not shown for clarity. Selected calculated bond distances [Å] and angles [deg]: Os–H1 1.618, Os–H2 1.588, Os–C 2.078, Os–N 2.112, Os–Cl 2.518, Os–P1 2.407, Os–P2 2.400, H1–Os–H2 54.7, H1–Os–Cl 78.6, H2–Os–C 70.7, N–Os–Cl 81.2, P1–Os–P2 163.1.

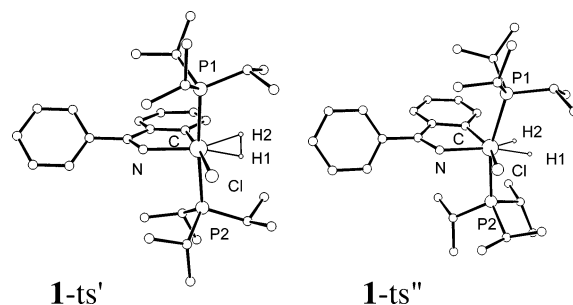


Figure 7. Theoretical transition-state structures **1-ts'** and **1-ts''**. C–H hydrogens are not shown for clarity.

c-1b and the molecule has no mirror plane; therefore the phosphorus atoms P1 and P2 are not equivalent. Rotational isomers *c-1a* and *c-1b* have very similar energies, the former being only slightly more stable (by 0.14 kcal/mol). The calculated H1–H2 distances in *c-1a* and *c-1b* are 1.460 and 1.472 Å, respectively.

DFT calculations were employed to study the observed dynamic processes in complex **1**. Two transition structures were located in this study, which are reported in Figure 7: one (**1-ts'**) for the process of H1/H2 exchange and another (**1-ts''**) for the process of PiPr_3 rotation. The transition structures **1-ts'** and **1-ts''** are 8.5 and 6.3 kcal/mol above the ground state *c-1a*, respectively. The geometry of **1-ts'** is approximately octahedral, and the H1–H2 distance is short at 0.90 Å. H1 and H2 are

(11) Castarlenas, R.; Esteruelas, M. A.; Gutierrez-Puebla, E.; Jean, Y.; Lledos, A.; Martin, M.; Tomas, J. *Organometallics* **1999**, *18*, 4296–4305.

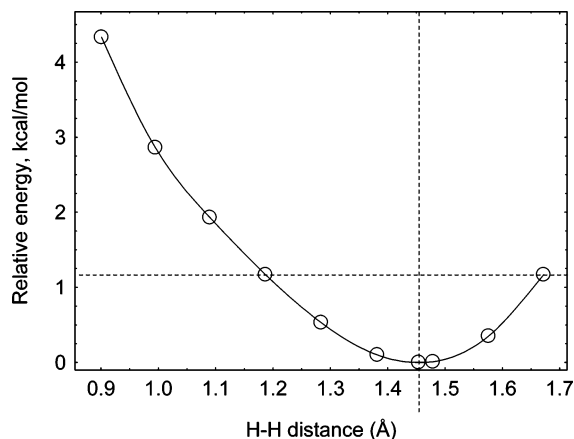


Figure 8. Relaxed *mPW1PW91/BS1* PES scan for *c-1a* carried out by varying the H1–Os–H2 angle.

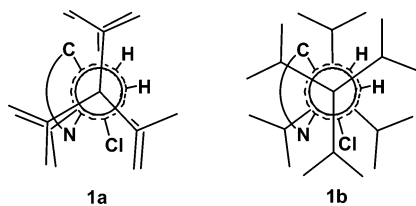
coplanar with P1 and P2 in *1-ts'*. The structure of *1-ts''* is related to those of *c-1a* and *c-1b* by rotation of PiPr_3 on P2.

A potential energy surface (PES) scan conducted by varying the H1–Os–H2 angle in *c-1a* produced a profile diagrammed in the plot of Figure 8, which shows that the H1–Os–H2 bending vibration (at ca. 917 cm^{-1}) is anharmonic and there is no second dihydrogen or dihydride tautomer coexisting with **1** on the PES.

Discussion

Low-temperature NMR spectroscopy suggests that complex **1** is a rapidly equilibrating mixture of two slightly different complexes in an approximately 55:45 ratio. The low-temperature ^{31}P NMR spectrum indicates that the predominant form of **1** has equivalent phosphine ligands. The minor species exhibits an AB pattern in the ^{31}P NMR, suggesting a structure with inequivalent phosphine ligands (see Figure 2).

DFT calculations demonstrate that the two subspectra exhibited by complex **1** result from hindered rotation around Os–P bonds. Rotameric structures consistent with these data are shown below, labeled as **1a** and **1b**. In both structures, the two hydride ligands are coplanar with the metal center and the N, C, and Cl ligand atoms. Structure **1a** has eclipsed $\text{P}(\text{iPr}_3)$ ligands, while structure **1b** has lower symmetry by virtue of a rotation of substituents around the Os–P2 bond. Structure **1b** has inequivalent phosphine ligands and is consistent with an AB pattern in the ^{31}P NMR spectrum.



Representations of the calculated structures for the two rotamers are depicted above in Newman projections. The Os atom is represented by the dashed circle. Consistent with the experimental observations, higher symmetry rotamer **1a** is calculated to be slightly more stable than rotamer **1b** (by 0.14 kcal/mol).

The low-temperature ^1H NMR spectrum of **1** in $\text{CDFCl}_2/\text{CDF}_2\text{Cl}$ (Figure 1) exhibits two pairs of resonances, which are assigned to the two rotamers **1a** and **1b**. Each structure has two inequivalent hydride environments. On the basis of their lower integrated intensity, the pair of resonances at -6.1 and -6.5

ppm are assigned to the minor rotamer **1b**. The resonances at -6.6 and -6.8 ppm are due to the major rotamer **1a**. Each structure has two chemically inequivalent hydride environments, which would lead to a total of four unique hydride signals. While this assignment is reasonable, attempts at detailed simulation of the NMR spectra as a function of temperature were not successful using the above chemical shifts as inputs (see below).

Since the high-temperature averaged spectrum exhibits $J_{\text{HD}} = 6.5$ Hz, heavily deuterated samples of **1** were prepared with a view to the detection of HD coupling in each of **1a** and **1b**. By using heavily deuterated samples, the spectrum of *1-d₁* can be observed with minimal interferences due to signals from **1**. This experiment gave an unexpected outcome. The expected four resonances were observed at very low temperature in the ^1H NMR spectrum, but HD coupling was too small to be resolved in the relatively broad signals. Surprisingly, the chemical shifts were quite different from those observed for **1**. There is ample precedent for isotope effects on the chemical shifts of polyhydride complexes upon deuteration. These effects are normally small, usually much less than 1 ppm. The changes in the hydride chemical shifts for **1** versus *1-d₁* amount to several ppm, which is beyond the range expected for normal isotope effects.

These observations suggest that the “true” hydride chemical shifts in complex **1** are those observed for *1-d₁*. In molecules such as **1**, two inequivalent hydrogen atoms related by a low barrier dynamic process can also exhibit quantum mechanical exchange coupling (QMEC) due to pairwise tunneling processes. There are several reports of this type of dynamic process in metal polyhydrides.¹² QMEC can lead to very large couplings and extreme second-order effects in the ^1H NMR spectrum of polyhydride complexes. Couplings of several thousand Hz have been reported in some cases.¹³ In the case of a two-spin AB system exhibited by the hydride signals in either **1a** or **1b**, a very large coupling can lead to a spectrum in which only the inner two lines of the four-line AB pattern are observable, with the intensity of the outer two lines being too low for detection. This explains the apparent extraordinary isotope effects on the hydride chemical shifts between **1** and *1-d₁*.

Analysis of the AB spin system presented by complex **1a** using the chemical shift data for *1a-d₁* gives a value of $J_{\text{AB}} = 9700$ Hz at 155 K. A similar analysis for **1b** gives $J_{\text{AB}} = 12\,000$ Hz (see Figure 4). In *1-d₁*, no exchange coupling is observed due to the reduction in the symmetry of the system. This is well preceded in the literature of QMEC and is a diagnostic for the occurrence of exchange coupling.

Incorporating exchange coupling in our simulations of the ^1H NMR spectra of **1** allows for complete simulation of the dynamic processes that are occurring and approximate estimation of the activation energy for the two dynamic processes exhibited by complex **1**. Observed and calculated spectra for a mixture of **1** and *1-d₁* at various temperatures are shown in Figure 4. The interchange of the two rotamers (**1a** and **1b**) has an activation energy $\Delta G^\ddagger = 7.8$ kcal/mol at 165 K. The interconversion of the two distinct hydride environments within molecules **1a** and **1b** has a slightly higher activation energy, $\Delta G^\ddagger = 8.5$ kcal/mol, at 165 K. These observed activation energies are in reasonable agreement with the barriers calculated using DFT. Within experimental error, no isotope effect on the

(12) Sabo-Etienne, S.; Chaudret, B. *Chem. Rev.* **1998**, *98*, 2077–2092.

(13) Chernega, A.; Cook, J.; Green, M. L. H.; Labella, L.; Simpson, S. J.; Souter, J.; Stephens, A. H. H. *J. Chem. Soc., Dalton Trans.* **1997**, 3225–3231.

rates is measurable. Deuteration has no effect on the rate of hydrogen atom permutation or on the rate of rotamer interconversion.

The observation of a large exchange coupling in complex **1** is consistent with a short distance (d_{HH}) between two hydrogen atoms that are linked by a low barrier exchange process. In a limited number of previous examples, it has been possible to study the temperature dependence of the exchange coupling and use this information in an empirical 2D harmonic oscillator model to determine d_{HH} .¹⁴ In the case of complex **1**, the barrier is quite low (ca. 8.5 kcal/mol), so we cannot observe static spectra over a wide range of temperatures. Thus we are unable to perform a full analysis of the exchange coupling as a function of temperature.

It is instructive to consider the existing experimental and computational results with respect to the H–H distance in complex **1**. The high-temperature averaged J_{HD} value for this molecule and the relaxation time data were previously interpreted in terms of $d_{\text{HH}} \cong 1.36$ Å. The reported relaxation time $T_{\text{1min}} = 49$ ms (300 MHz). If this relaxation is attributed entirely to the hydride–hydride dipolar interaction, this leads to $d_{\text{HH}} = 1.36$ Å. If the minor contributions to relaxation from adjacent spin-active nuclei in **1** are included using structure *c-1a* as a guide, a more accurate value of $d_{\text{HH}} = 1.41$ Å is obtained.¹⁵ This value is in reasonable agreement with the computed value of $d_{\text{HH}} = 1.46$ Å from the minimum in the PES scan (Figure 8). The latter value is similar to the corresponding distance of 1.48 Å calculated by Esteruelas and co-workers for the simple model $\text{OsH}_2\text{Cl}\{\text{NH}=\text{C}(\text{H})\text{C}_6\text{H}_4\}(\text{PH}_3)_2$.⁵ It should be noted that the experimental value of T_{1min} is a vibrational average, and in the case of complex **1** it is dominated by the distances shorter than 1.46 Å because the PES is less steep in that direction. Therefore, the experimental distance derived from the T_{1min} is

(14) Heinekey, D. M.; Hinkle, A. S.; Close, J. D. *J. Am. Chem. Soc.* **1996**, *118*, 5353–5361.

(15) Gusev, D. G. *J. Am. Chem. Soc.* **2004**, *126*, 14249–14257.

naturally slightly shorter than the one corresponding to the true electronic minimum of the system.

An independent indicator of d_{HH} is provided by measurement of $J_{\text{HD}} = 6.5$ Hz in **1-d**₁. Several empirical correlations between d_{HH} and J_{HD} have been reported.¹⁶ For longer H–H distances, the more reliable approach is the correlation of Gelabert et al.,¹⁷ which suggests that $J_{\text{HD}} = 6.5$ Hz is consistent with $d_{\text{HH}} = 1.52$ Å.

Thus DFT calculations and two independent experimental methods suggest that the HH distance in complex **1** is ca. 1.5 Å. This is quite consistent with the occurrence of a very substantial exchange coupling, as observed.

Conclusion

Very low-temperature NMR spectroscopy and DFT calculations show that the structure of complex **1** presents a much more complex situation than previously thought. Hindered phosphine rotation leads to two slightly different rotational isomers of **1** in rapid dynamic equilibrium. In each rotamer, the hydride ligands are readily delocalized in a soft potential, which leads to QMEC, manifested by very large and temperature-dependent values of the coupling constant between the hydride atoms. The previously reported H–H distance for complex **1** of 1.36 Å should be revised to ca. 1.46 Å. The structure of complex **1** is best described as a compressed dihydride complex.

Acknowledgment. This research was supported by the National Science Foundation. N.S. is grateful to the Deutsche Forschungsgemeinschaft for a postdoctoral fellowship.

OM060284H

(16) Heinekey, D. M.; Lledos, A.; Lluch, J. M. *Chem. Soc. Rev.* **2004**, *33*, 175–182.

(17) Gelabert, R.; Moreno, M.; Lluch, J. M.; Lledos, A.; Pons, V.; Heinekey, D. M. *J. Am. Chem. Soc.* **2004**, *126*, 8813–8822.